2020 IEEE International Conference on Robotics and Automation (ICRA)
31 May - 31 August, 2020. Paris, France

Real-Time Robot Reach-To-Grasp Movements Control Via EOG and EMG Signals Decoding

Bernhard Specht[1] *, Zied Tayeb[1] *, Emannual Dean[1], Rahil Soroushmojdehi[2], and Gordon Cheng[1]

Abstract— **In this paper, we propose a real-time human-robot interface (HRI) system, where Electrooculography (EOG) and Electromyography (EMG) signals were decoded to perform reach-to-grasp movements. For that, five different eye movements (up, down, left, right and rest) were classified in real-time and translated into commands to steer an industrial robot (UR-10) to one of the four approximate target directions. Thereafter, EMG signals were decoded to perform the grasping task using an attached gripper to the UR-10 robot arm. The proposed system was tested offline on three different healthy subjects, and mean validation accuracy of 93.62% and 99.50% were obtained across the three subjects for EOG and EMG decoding, respectively. Furthermore, the system was successfully tested in real-time with one subject, and mean online accuracy of 91.66% and 100% were achieved for EOG and EMG decoding, respectively. Our results obtained by combining real-time decoding of EOG and EMG signals for robot control show overall the potential of this approach to develop powerful and less complex HRI systems. Overall, this work provides a proof-of-concept for successful real-time control of robot arms using EMG and EOG signals, paving the way for the development of more dexterous and human-controlled assistive devices.**

I. INTRODUCTION

Over the last decades, human-robot interaction for rehabilitation and assistance has gained momentum [1] and has continuously attracted many researchers and industrial companies [2]. Highly autonomous robots have been used in multiple industrial applications, such as disassembling tasks and robot-cranes [3]. Apart from industrial sections, robots have been utilized in different healthcare applications. For instance, nursing robots [4], robots in gait rehabilitation for patients after stroke [5] and assistive telepresence robots for elderly [6] have been widely used. Despite the tremendous advances that have been made, various problems persist [7] and the development of human-robot interfaces (HRI) still needs further investigation of the capabilities of human-robot collaboration when designing the interface to produce desirable actions [8]. Many researchers have been working on incorporating human bio-signals, as one of the most important input signals that can be used to control assistive robots [9]. Assistive robotics using signals that are acquired from muscle activity (EMG) [10], brain activity (EEG) [11] and eye movements (EOG) [12], [13], [14], [15] have shown promising results. However, these systems still exhibit some drawbacks, such as complex and expensive experimental setups, which makes transferring this into commercial products a challenging task [16]. Along the same lines, using one unique signal for robot control limits the number of degrees of freedom (DoF) that can be controlled. In this context, many studies have been recently focusing on combining multiple bio-signals to increase the number of DoF when controlling assistive robots [17]. This has therefore spurred research in designing hybrid HRI systems [18]. In [19], authors integrated EOG, and evoked related potentials. A comparison between different modes of robot control including accelerometer data, EOG + EMG, EOG + blink and EOG + ERD/ERS + blink in [16] showed that combining EOG and EMG offers a good compromise between accuracy, ease-of-use, and number of DoFs for robot control. Recent work by Zhang et al. combined EEG/EMG/EOG-Based Multimodal Human-Machine Interface to control a soft robot-hand in real-time [20]. The core contribution of the work resides in designing an effective and powerful HRI system based on real-time EMG and EOG decoding for real-time control of different reach-to-grasp movements. Although many previous studies have investigated combining EEG and EMG signals for robot control [21], [22], [23], [24], EEG signal still exhibits many problems and limitations, such as low spatial resolution limiting the number of the control commands that can be decoded [25] as well as low to signal-noise ratio making them impracticable to use in daily-life scenarios. Thus, substituting EEG by EOG signals is thought to offer a better solution for more robust and real-time human-robot interaction. In this work, we underpin the real-time capabilities of the proposed system by demonstrating the successful online control of a UR-10 robot arm (universal-robots). Our system (shown in Figure 1) can be extended to classify more complex movements, en route to designing a powerful, effective and reliable HRI for disabled and elderly people. The remainder of this paper is structured as follows: the first section describes the designed experimental paradigms as well as data acquisition, the second section shows offline EOG and EMG classification, the third section describes the real-time signal decoding, the real-time setup as well as the robot control part are described in section 4, and we enumerate the strengths and weaknesses of the designed system and propose possible future improvements in the last section.

*This work was supported in part by Ph.D. grant of the German Academic Exchange Service (DAAD).

[1] The institute for cognitive systems, Technical University of Munich, Arcisstraße 21, 80333 München, Germany zied.tayeb@tum.de

[2] Department of Electronics, Information and Bioengineering, Politecnico di Milano, Milan, Italy (rahil.soroushmojdehi@mail.polimi.it).

* Both authors contributed equally to this manuscript.

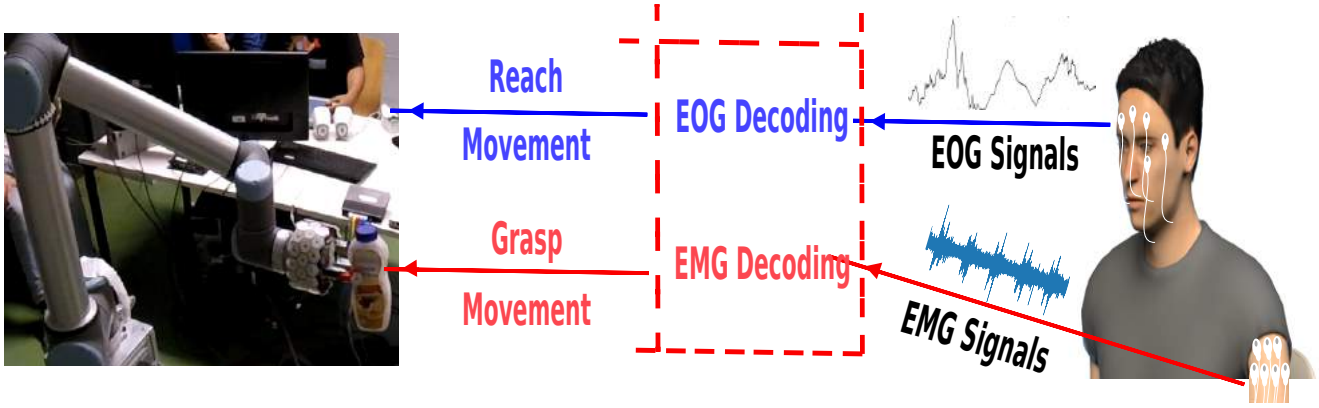

Fig. 1. Overview of the real-time developed HRI system. EMG and EOG signals were decoded in real-time and the decoded information was translated intol commands to control a UR-10 robot in order to perform complex reach-to-grasp movements.

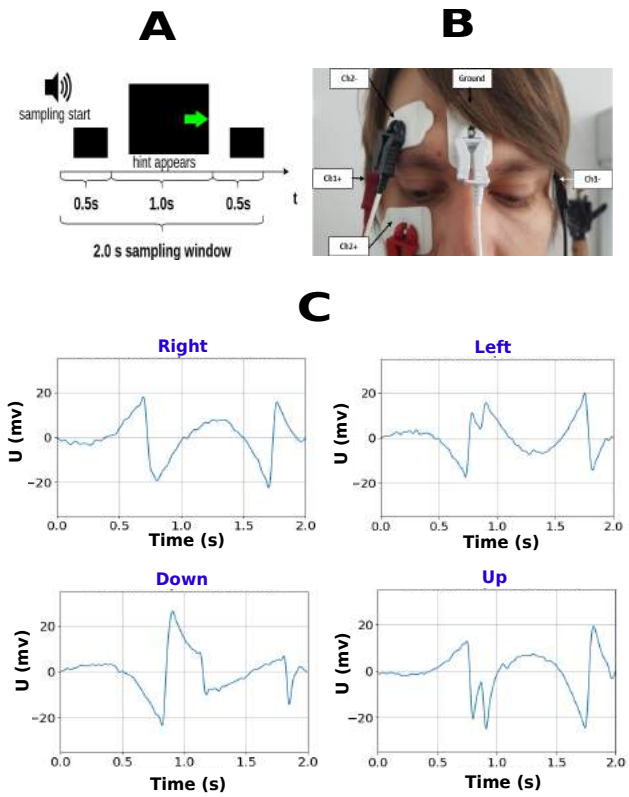

Fig. 2. **A** shows the paradigm for recording trials used to train the EOG classifiers. For each trial, a window of two seconds is sampled. For the first half second the screen is black, then a uniformly selected cue in the form of an arrow appears at the position where the subject is expected to look at, or the screen stays empty for classification of relaxation. The cue disappears after one second and is followed by a black screen for another half of a second. A short tone marks the start of a sampling period. **B** shows the electrode placement on the subject. One ground electrode was placed in the middle of the forehead. The electrodes CH1+ and CH1- were placed on the right of the subject's right eye and left of the subject's left eye respectively. CH2+ and CH2- were placed on beneath and on top of the subject's right eye. **C** shows the filtered subtracted signals of the horizontally placed electrodes for left and right eye movements and the vertically placed electrodes for up and down eye movements.

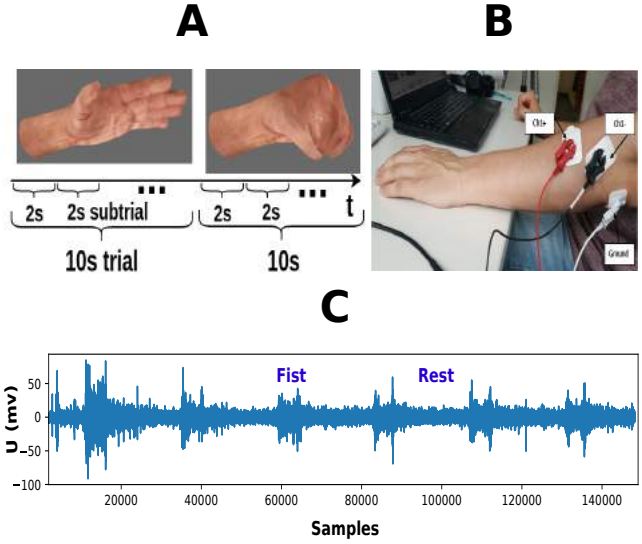

Fig. 3. **A** shows the animations with timings of two consecutive trials showed to the subject while recording EMG signals. A trial is divided into five sub-trials, where each trial is recorded as a sampling window of two seconds. **B** shows the electrode placement for the EMG recording. The ground electrode was placed on the elbow. Two electrodes CH1+ and CH2+ were placed on top of the forearm forming a channel for bipolar recording. **C** shows recorded EMG data. When the subject forms a fist higher activity can be observed.

II. Methods

A. EOG & EMG signals recording and acquisition

EOG and EMG signals were recorded from three healthy subjects (two males and one female) using the g.USBamp system (G.tec medical engineering GMBH, Austria) with a sampling frequency of 1200 Hz. Subjects were between 22 and 27 years old and claimed to have no record of neurological disorders. The three subjects were recruited to perform four different eye movements (up, down, left, and right) by following a pointing arrow on the screen during the training phase (EOG task), as well as to perform one hand movement, namely power-fist followed by a relaxation phase.

The pointing arrow (cue) was randomly displayed and was selected from a discrete uniform distribution. All recording sessions took place in the lab and yielded a total of 150 and 400 trials for EOG and EMG signals, respectively. For EOG signals, 30 trials for each direction were recorded (including the rest phase/no movement) forming the total number of 150 trials. For EMG, 200 trials for each condition (power-fist vs rest) were collected yielding to the total number of 400 trials. One pair of electrodes, which cover the muscles of the forearm (flexor and extensor carpi radialis) in a ring-like fashion were used, and the reference electrode was placed on the elbow bone. It should be noted that liquid-gel ECG electrodes (model: 5048 mm) were used for EMG recording. The open source library mushu [26] was used for data acquisition and both EMG and EOG signals were thereafter processed using the gumpy.signal module in the gumpy BCI toolbox [21]. For that, EOG signals were band-pass filtered between 1 and 22 Hz using a 4th order zero-phase Butterworth filter, whereas EMG was band-pass filtered between 30 and 500 Hz using the same filter. Both signals were notch filtered at 50 Hz to remove the power line interference [21]. The designed experimental paradigms, electrode placement and recorded signals for EOG and EMG are shown in Figure 2 and Figure 3, respectively.

III. Results

A. Offline results: EOG data classification

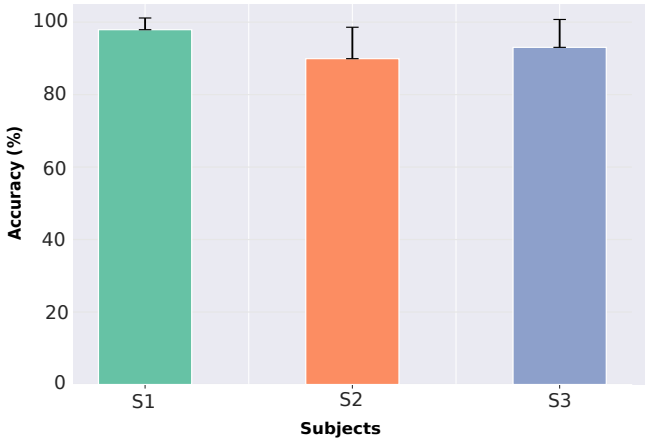

Fig. 4. Bar plot showing the mean validation accuracy for each subject with the standard deviation.

1) EOG signal classification: Filtered EOG signals were analyzed using two sliding windows (from 0.0s to 1.5s, and from 0.5s to 2s). The length of the sliding window was chosen for the purpose of allowing real-time control. For each sliding window of 1.5s, four different features, namely minimum value, maximum value, variance and threshold crossing count (crossing positive and negative threshold) were extracted and were used for training, as well as for the movement classification in real-time. A feature selection algorithm (SFSF) [27] was used and trained to select the best

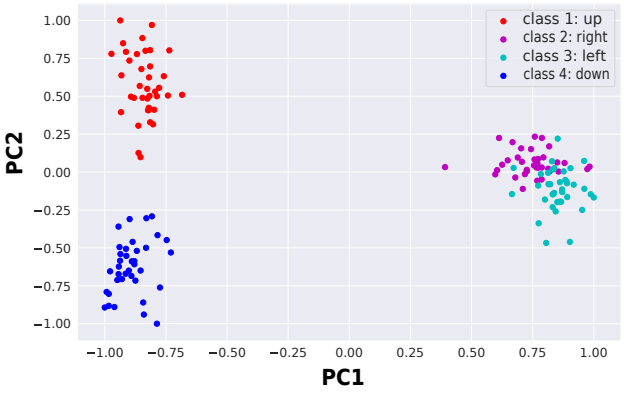

Fig. 5. Feature space showing the different eye movement trials after performing PCA.

features (a subset of the initial features) using a 10-fold cross validation. Only the selected features were then used to train a k-nearest neighbors (KNN) classifier. We wish to mention that two different KNN models were trained to classify EOG signals. The first one was served for detecting if there is an eye movement or not (rest vs eye movement). If an eye movement was detected, a second classifier was trained to classify the different directions of eye movement (up, left, right, or down), and hence deciding on the robot's target direction. It is worth noting that 10-fold cross-validation was used during the validation phase to evaluate the model's performance. Figure 4 shows the classification results for the three different subjects. Overall, we achieved an average success rate of $97.91\% \pm 3.22\%$, $89.92\% \pm 8.66\%$ and $93.04\% \pm 7.69\%$ for the three subjects, respectively, yielding a mean accuracy of 93.62% across the three subjects, when recognizing the different eye movements. A principal component analysis (PCA) was performed (n_components=2) to visualize the different classes and results are depicted in Figure 5, which shows that most eye movements trials are highly separable, except the left and right which were also confused during the real-time test. It should be mentioned that the mean balanced accuracy (bACC), where the average of correct predictions for each class was computed and used.

B. EMG signal classification

The mean absolute value and the sum of absolute discrete differences were used to extract features from EMG signals. Those two features were extracted from different consecutive overlapping windows within a time window of two seconds. The overlapping windows had a size of 0.2 seconds and overlapped with their neighbors for 0.04 seconds. The same sequential feature selector algorithm was used to choose features for training a KNN classifier with 10 fold cross-validation. As this is a binary EMG classification task, signals were correctly classified during the validation as well as in the test phase with 100% accuracy.

C. Real-time signals decoding

After the validation of the proposed system offline, we used a UR-10 robot with an attached gripper to test the

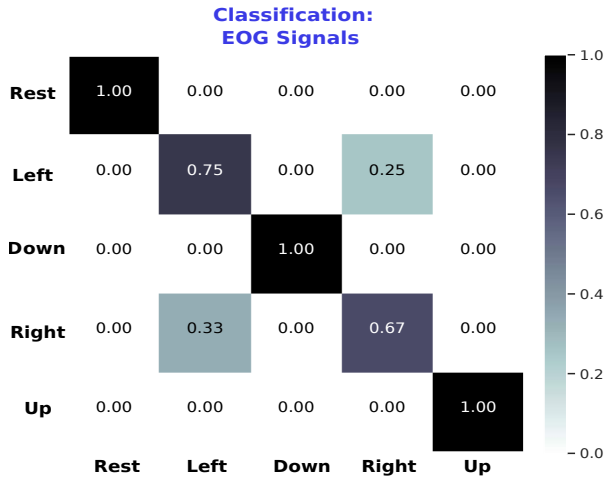

Fig. 6. Confusion matrix for the real-time test showing that left and right were the only classes confused during the online phase.

proposed system online. For that, the subject had to perform one of the four different eye movements to control the robot to perform a reach movement as described in table I. EOG signals are acquired in real-time, processed, classified using the saved offline model and decoded information was thereafter translated into commands to move the UR-10 robot towards the right direction (an online demo is shown in the supplementary video S1). Once the robot reaches the target object, the subject flexes his muscles, EMG signals are processed, classified in real-time using the saved EMG classifier and the attached gripper to the UR-10 robot arm performed the grasping task. Overall, an online accuracy of 91.66% and 100% were, respectively, obtained when classifying EOG and EMG signals using one single subject. The confusion matrix in Figure 6 shows that down and up eye movements were always correctly classified, whereas the left and right movements were sometimes confused during the test phase. For the EMG online classification, all performed fist movements were correctly classified. Table I summarizes robot's and subject's different actions.

TABLE I
SUBJECT ACTION TO ROBOT ACTION MAPPING

Signal	Subject's Action	Robot's Action [$P(i)$&$G(j)$]
EOG	look left	move up left
	look up	move up right
	look right	move down right
	look down	move down left
	rest (idle state)	no movement
EMG	grasp	close gripper
	relax	open gripper

D. Robot interface

The robot interface used to connect the *Decoder* with the robot controller is depicted in Figure 7. The *Decoder* uses two ros-clients to trigger the *Robot's Actions*, namely *Reach Movements* $P(i)$and *Gripper States* $G(j)$. In the case

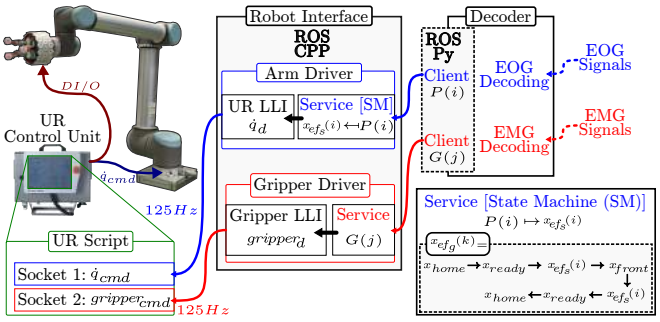

Fig. 7. Robot Interface: The robot interface to control the robot's actions is implemented in ROS, where two ROS services have been implemented. The first one to control the arm motions, using a State Machine SM, and the second one to trigger the gripper states (open/close). The EOG decoder executes the *Reach Movements* $P(i)$, and the EMG triggers the *Gripper States* $G(j)$. The *Reach Movements* are divided into a sequence of end-effector positions ($x_{efg}(k)$) triggered by a *State Machine*.

of $G(j)$, the client triggers two possible gripper actions *open* and *close*. These actions are directly transformed into gripper commands by the *Gripper Driver*, which, in turn, are transformed into digital outputs (DI/O) by the UR-Script running in the UR-Control Unit. For the Arm actions, the *Decoder* selects a specific *Reach Movement* $P(i)$ using the classification of the EOG signals. The selected $P(i)$ is sent to the *Arm Driver* using a ros-client. The ros-service implemented in the *Robot Interface* maps the desired $P(i)$ into a predefined end-effector state (end-effector position $x_{efs}(i)$). This position $x_{efs}(i)$ is used in a *State Machine* (SM) to trigger the different end-effector goals $x_{efg}(k)$. These goals are used as desired positions in a Cartesian controller. Then, the output of the Cartesian controller is transformed into joint velocity commands [28] and sent to the robot using the UR-Script.

1) Cartesian Control: To control the robot end-effector, we implemented a second order sliding mode controller in the Cartesian space defined as:

$$\tau = -K_d S_q + Y_r \Theta \in \mathbb{R}^n \tag{1}$$

where $K_{d_+} = K_{d_+}^T \in \mathbb{R}^n$ and $Y_r\Theta \in \mathbb{R}^n$ is the robot regressor. The joint error surface S_q is defined as:

$$S_q = \dot{q} - \dot{q}_r \in \mathbb{R}^n \tag{2}$$

where the joint velocity reference $\dot{q}_r \in \mathbb{R}^n$ is given as:

$$\dot{q}_r = J(q)^{-1}\dot{x}_r \tag{3}$$

and the Cartesian velocity reference $\dot{x}_r$ is given as:

$$\dot{x}_r = \dot{x}_d - K_p \Delta x + S_d - K_{i_1} \int_{t_0}^{t} S_\delta d\zeta - K_{i_2} \int_{t_0}^{t} \tanh(\mu S_\delta)\, d\zeta \tag{4}$$

with $\tanh(\mu\bullet)$ as a smooth approximation for the function $sign(\bullet)$, and $\mu > 0 \in \mathbb{R}$. $K_p, K_{i_j} > 0 \in \mathbb{R}^{6\times 6}$, $j = 1, 2$. The Cartesian error manifold S_δ is

$$S_\delta = S - S_d = (\Delta\dot{x} + K_p \Delta x) - \left(S(t_0)\, e^{-\kappa t}\right) \tag{5}$$

with the Cartesian position error defined as:

$$\Delta x = x - x_d \in \mathbb{R}^6 \tag{6}$$

where $\Delta\dot{x} = \dot{x} - \dot{x}_d$ is the Cartesian velocity error, where x_d and $\dot{x}_d$ stands for the desired Cartesian pose and velocity, respectively. The desired Cartesian pose $x_d \in \mathbb{R}^6$ is composed of a desired position vector x_{ef_d} and a desired orientation vector $\theta_{ef_d} \in \mathbb{R}^3$, which is obtained using the *Euler angles* representation *Z-Y-X*. In our particular case, the goal is to keep the orientation of the end-effector constant, i.e. $\theta_{ef_d}(t) = \theta_{ef}(0)$. The position of the end-effector depends on the *Reach Movement* $P(i)$ triggered by the EOG/EMG Decoder. The discrete movement obtained from $P(i)$ is transformed into a set of end-effector goals $x_{ef_g}(k) \in \mathbb{R}^3$, where k is defined by the State Machine SM, see Figure 7. Then, we generate a continuous desired trajectory using a spline function for each $x_{ef_g}(k)$.

2) Spline End-Effector Trajectory x_{ef_d}: To generate a smooth trajectory from the initial desired Cartesian position $x_{ef_i} \in \mathbb{R}^3$ to the goal position $x_{ef_g}(k)$, we employ the following trajectory generator:

$$x_{ef_d} = a_1\bar{x}_{ef} + x_{ef_i},\ \dot{x}_{ef_d} = a_2\bar{x}_{ef} \tag{7}$$

where $\bar{x}_{ef} = x_{ef_g}(k) - x_{ef_g}(k-1)$, with $x_{ef_g}(0) = x_{ef_i} = x_{home}$.

The coefficients a_i are defined as: $a_1 = 10r^3 - 15r^4 + 6r^5$, $a_2 = (30r^2 - 60r^3 + 30r^4)/(t_f)$ and $a_3 = (60r - 180r^2 + 120r^3)/(t_f^2)$, where $r = t/t_f$ is a time ratio between the current time t and the desired total time t_f. This function guarantees a smooth trajectory that satisfies the constraints $x_{ef_d}(0) = x_{ef_g}(k-1)$, $x_{ef_d}(t_f) = x_{ef_g}(k)$ and $\dot{x}_{ef_d}(0) = \dot{x}_{ef_d}(t_f) = \ddot{x}_{ef_d}(0) = \ddot{x}_{ef_d}(t_f) = 0 \in \mathbb{R}^3$. The discrete movements $P(i)$ are a set of predefined Cartesian positions $x(i) \in \mathbb{R}^3$. The robot's end-effector continuous trajectory $\chi(t)$ is generated using polynomial interpolation between two positions u and v of that set, see eq. (11).

$$r = \frac{t - t_0}{\Delta t} \tag{8}$$

$$\Delta t = t_f - t_0 \tag{9}$$

$$p(t) = 35r^4 - 84r^5 + 70r^6 - 20r^7 \tag{10}$$

$$\chi(t) = p(t)\Delta x(k) + x(v), \tag{11}$$

with t_0 and t_f as the initial and final time for the trajectory, and Δt defines the total time of the trajectories, in our case, it was set to $10s$. $\Delta x(k) = x(u) - x(v)$, where the indices u, v are the *target* defined by the SM, depending on the desired action. Each action takes $30s$ since the robot has to move to three different stations, namely, *home*, *reach*, and *target*.

IV. Discussion

In this work, we propose a human-robot interface based on EMG and EOG decoding to control reach-to-grasp movements of a UR-10 robot arm. Overall, our results show that we could successfully classify both signals with more than 90% accuracy across three different subjects and we underpin the real-time aspect by showing the successful online control of the robot arm. To the best of our knowledge, this experiment is among the very few, if not the only one, to demonstrate the real-time control of robot arms using decoded information from EMG and EOG signals. Nonetheless, the proposed system still has some limitations that should be addressed in future work, in order to investigate to what extent this approach could be generalized across many subjects, including elderly and disabled people, to further verify the robustness of such a system when used in real-life scenarios, as well as to extend the proposed approach to classify more complex reach-to-grasp movements.

A. Limitations

First, this experiment was solely tested on healthy subjects and no experiments with elderly or disabled people were performed. Hence, it remains questionable whether a similar performance could be obtained when testing with patients. Furthermore, we wish to mention that the subject had to be trained to correctly and repetitively perform the different eye movements prior to the recording. Therefore, generalizing the developed approach across many subjects would be a challenging task. Aside from that, we noticed that sweat or slight changes in the electrode's position during recording and the difference between muscle tissues of the participants drastically decreased the quality of the recorded sEMG signal and therefore deteriorate classification accuracy. For example, the classification accuracy dropped significantly when testing on the female participant (subject 2 in our analysis) and a validation accuracy of only 89.92% was attained compared to more than 97% and 93% for subjects 1 and 3, respectively.

B. Future work

Overall, the proposed system presents a proof-of-concept for the development of a powerful human-robot interface, which relies on the combination of EOG and EMG decoding to steer an industrial robot arm to perform reach-to-grasp movements, such as grasping and sorting objects in a shelf. As future work, we will consider using the proposed system to classify additional eye movements (e.g. blinking) and extra hand gestures from EMG signals, and hence increase the total number of control commands of the robot. Aside from that, the gel-based electrodes used in the experiments were reported by the three subjects as uncomfortable for long-term use. That's why we are currently performing other experiments with new customized, stretchable graphene sensors (human skin-like sensors), which can increase durability and wearability [29] [30]. Last, as the proposed system does not provide any sensory feedback to the user about the grasped object, such as temperature or stiffness, it would be important to investigate the artificial robot skin [31] capabilities to close the loop from controlling to feeling. Thus, integrating such technologies with our proposed approach could make such a system more practical and hence speed up the development of more powerful and reliable HRI and brain-computer interface systems.

V. Conclusions

This paper proposes a human-robot interface system based on the real-time decoding of EOG and EMG signals to

control reach-to-grasp movements using an industrial UR-10 robot arm. The system was tested with three different healthy subjects in the validation phase and one subject during the online phase. Overall, we obtained a mean validation accuracy of 93.62% and 99.50% for EOG and EMG classification, respectively, and online accuracy of 91.66% and 100% during the online phase. We demonstrate the real-time capability of the proposed system by showing successful control of the robot arm using decoded information from both signals.

VI. Source code and documentation

All source code of this work is released under the MIT license and is made publicly available under `https://github.com/spebern/eog-emg`.

References

[1] P. Beckerle, G. Salvietti, R. Unal, D. Prattichizzo, S. Rossi, C. Castellini, S. Hirche, S. Endo, H. B. Amor, M. Ciocarlie, *et al.*, "A human–robot interaction perspective on assistive and rehabilitation robotics," *Frontiers in neurorobotics*, vol. 11, 2017.

[2] T. Meneweger, D. Wurhofer, V. Fuchsberger, and M. Tscheligi, "Working together with industrial robots: Experiencing robots in a production environment," in *2015 24th IEEE International Symposium on Robot and Human Interactive Communication (RO-MAN)*. IEEE, 2015, pp. 833–838.

[3] A. Tellaeche, I. Maurtua, and A. Ibarguren, "Human robot interaction in industrial robotics. examples from research centers to industry," in *2015 IEEE 20th Conference on Emerging Technologies & Factory Automation (ETFA)*. IEEE, 2015, pp. 1–6.

[4] T. Tanioka, K. Osaka, R. Locsin, Y. Yasuhara, and H. Ito, "Recommended design and direction of development for humanoid nursing robots perspective from nursing researchers," *Intelligent Control and Automation*, vol. 8, no. 02, pp. 96–110, 2017.

[5] D. R. Louie and J. J. Eng, "Powered robotic exoskeletons in post-stroke rehabilitation of gait: a scoping review," *Journal of neuroengineering and rehabilitation*, vol. 13, no. 1, 2016.

[6] S. Koceski and N. Koceska, "Evaluation of an assistive telepresence robot for elderly healthcare," *Journal of medical systems*, vol. 40, no. 5, 2016.

[7] T. B. Sheridan, "Human–robot interaction: status and challenges," *Human factors*, vol. 58, no. 4, pp. 525–532, 2016.

[8] M. A. Goodrich, A. C. Schultz, *et al.*, "Human–robot interaction: a survey," *Foundations and Trends® in Human–Computer Interaction*, vol. 1, no. 3, pp. 203–275, 2008.

[9] S. Goto, O. Yano, Y. Matsuda, T. Sugi, and N. Egashira, "Development of hands-free remote operation system for a mobile robot using eog and emg," *Electronics and Communications in Japan*, vol. 100, no. 10, pp. 38–47, 2017.

[10] L.-Z. Liao, Y.-L. Tseng, H.-H. Chiang, and W.-Y. Wang, "EMG-based control scheme with SVM classifier for assistive robot arm," in *2018 International Automatic Control Conference (CACS)*. IEEE, 2018, pp. 1–5.

[11] N. M. Krishnan, M. Mariappan, K. Muthukaruppan, M. H. A. Hijazi, and W. W. Kitt, "Electroencephalography (EEG) based control in assistive mobile robots: A review," in *IOP Conference Series: Materials Science and Engineering*, vol. 121, no. 1. IOP Publishing, 2016.

[12] Q. Huang, Y. Chen, Z. Zhang, S. He, R. Zhang, J. Liu, Y. Zhang, M. Shao, and Y. Li, "An EOG-based wheelchair robotic arm system for assisting patients with severe spinal cord injuries," *Journal of neural engineering*, 2019.

[13] X. Guo, W. Pei, Y. Wang, Y. Chen, H. Zhang, X. Wu, X. Yang, H. Chen, Y. Liu, and R. Liu, "A human-machine interface based on single channel EOG and patchable sensor," *Biomedical Signal Processing and Control*, vol. 30, pp. 98–105, 2016.

[14] A. Bulling, D. Roggen, and G. Tröster, "Wearable EOG goggles: Seamless sensing and context-awareness in everyday environments," *Journal of Ambient Intelligence and Smart Environments*, vol. 1, no. 2, pp. 157–171, 2009.

[15] Q. Huang, S. He, Q. Wang, Z. Gu, N. Peng, K. Li, Y. Zhang, M. Shao, and Y. Li, "An EOG-based human–machine interface for wheelchair control," *IEEE Transactions on Biomedical Engineering*, vol. 65, no. 9, pp. 2023–2032, 2017.

[16] L. Minati, N. Yoshimura, and Y. Koike, "Hybrid control of a vision-guided robot arm by EOG, EMG, EEG biosignals and head movement acquired via a consumer-grade wearable device," *Ieee Access*, vol. 4, pp. 9528–9541, 2016.

[17] Y. Nam, B. Koo, A. Cichocki, and S. Choi, "GOM-face: GKP, EOG, and EMG-based multimodal interface with application to humanoid robot control," *IEEE Transactions on Biomedical Engineering*, vol. 61, no. 2, pp. 453–462, 2013.

[18] e. a. DelPreto, Joseph, "Plug-and-play supervisory control using muscle and brain signals for real-time gesture and error detection." in *Robotics: Science and Systems XIV, Robotics: Science and Systems Foundation*, 2018.

[19] J. Ma, Y. Zhang, A. Cichocki, and F. Matsuno, "A novel EOG/EEG hybrid human–machine interface adopting eye movements and erps: Application to robot control," *IEEE Transactions on Biomedical Engineering*, vol. 62, no. 3, pp. 876–889, 2014.

[20] J. Zhang, B. Wang, C. Zhang, Y. Xiao, and M. Y. Wang, "An EEG/EMG/EOG-based multimodal human-machine interface to real-time control of a soft robot hand," *Frontiers in neurorobotics*, vol. 13, 2019.

[21] Z. Tayeb, N. Waniek, J. Fedjaev, N. Ghaboosi, L. Rychly, C. Widderich, C. Richter, J. Braun, M. Saveriano, G. Cheng, and J. Conradt, "Gumpy: a python toolbox suitable for hybrid brain–computer interfaces," *Journal of Neural Engineering*, vol. 15, no. 6, 2018.

[22] R. Leeb, H. Sagha, R. Chavarriaga, and J. d. R. Millán, "A hybrid bci based on the fusion of EEG and EMG activities," *Journal of Neural Engineering*, vol. 8, pp. 225–9, 2011.

[23] Y. Li, J. Long, T. Yu, Z. Yu, C. Wang, H. Zhang, and C. Guan, "An EEG-based BCI system for 2-D cursor control by combining Mu/Beta rhythm and P300 potential," *IEEE Transactions on Biomedical Engineering*, vol. 57, no. 10, pp. 2495–2505, 2010.

[24] Y. Li, J. Pan, F. Wang, and Z. Yu, "A hybrid BCI system combining P300 and SSVEP and its application to wheelchair control," *IEEE Transactions on Biomedical Engineering*, vol. 60, no. 11, pp. 3156–3166, 2013.

[25] M. A. Lebedev and M. A. L. Nicolelis, "Brain-machine interfaces: From basic science to neuroprostheses and neurorehabilitation." *Physiol Rev*, vol. 97, no. 2, pp. 767–837, 2017.

[26] B. Venthur and B. Blankertz, "Mushu, a free- and open source bci signal acquisition, written in python," in *Engineering in Medicine and Biology Society (EMBC), 2012 Annual International Conference of the IEEE*. IEEE, Aug 2012, pp. 1786–1788.

[27] S. Aungsakul, A. Phinyomark, P. Phukpattaranont, and C. Limsakul, "Evaluating feature extraction methods of electrooculography (eog) signal for human-computer interface," *Procedia Engineering*, vol. 32, pp. 246–252, 2012.

[28] E. Dean-Leon, F. Bergner, K. Ramirez-Amaro, and G. Cheng, "From multi-modal tactile signals to a compliant control," in *2016 IEEE-RAS 16th International Conference on Humanoid Robots (Humanoids)*, Nov 2016, pp. 892–898.

[29] S. K. Ameri, M. Kim, I. A. Kuang, W. K. Perera, M. Alshiekh, H. Jeong, U. Topcu, D. Akinwande, and N. Lu, "Imperceptible electrooculography graphene sensor system for human–robot interface," *npj 2D Materials and Applications*, vol. 2, no. 1, 2018.

[30] J. A. Rogers, "Wearable electronics: Nanomesh on-skin electronics," *Nature nanotechnology*, vol. 12, no. 9, 2017.

[31] F. Bergner, E. Dean-Leon, and G. Cheng, "Event-based signaling for large-scale artificial robotic skin - realization and performance evaluation," in *2016 IEEE/RSJ International Conference on Intelligent Robots and Systems (IROS)*, 2016, pp. 4918–4924.